Global radiosonde balloon drift statistics

Dian J. Seidel,[1] Bomin Sun,[2] Michael Pettey,[2] and Anthony Reale[3]

Received 10 August 2010; revised 10 January 2011; accepted 20 January 2011; published 7 April 2011.

[1] The drift of radiosonde balloons during their ascent has generally been considered a negligible factor in applications involving radiosonde observations. However, several applications envisioned for observations from the Global Climate Observing System (GCOS) Reference Upper Air Network (GRUAN) require estimates of balloon drift. This study presents a comprehensive global climatology of radiosonde balloon drift distance and ascent time, based on 2 years of data from 419 stations, with particular attention to GRUAN stations. Typical drift distances are a few kilometers in the lower troposphere, ~5 km in the midtroposphere, ~20 km in the upper troposphere, and ~50 km in the lower stratosphere, although there is considerable variability due to variability in climatological winds. Drift distances tend to increase with height above the surface, be larger in midlatitudes than in the tropics, be larger in winter than in summer, and vary with wind (and consequent balloon drift) direction. Most estimates of elapsed time from balloon launch to various pressure levels, due to vertical balloon rise, have median values ranging from about 5 min at 850 hPa to about 1.7 h at 10 hPa, with ranges of about 20% of median values. Observed elapsed times exceed those estimated using assumed 5 or 6 m/s rise rates.

Citation: Seidel, D. J., B. Sun, M. Pettey, and A. Reale (2011), Global radiosonde balloon drift statistics, *J. Geophys. Res.*, *116*, D07102, doi:10.1029/2010JD014891.

1. Introduction and Motivation

[2] Temperature and humidity observations from radiosondes are quintessentially point measurements that, in the absence of observational biases, represent instantaneous atmospheric conditions at the locations of the balloon-borne sensors. However, it is often assumed that they represent conditions over larger regions, for example in: comparisons with observations from ground-based or satellite-mounted instruments; evaluations of model representations or predictions of atmospheric profiles; estimation of average profile values using data from multiple launches from one or more ground stations; and evaluation of variability and trends in profiles from a time series of observations from a site.

[3] The validity of these applications depends on the spatial representativeness of radiosonde observations, which is mainly a function of two things: the spatial structure of the atmosphere and the horizontal drift of the ascending balloon and instrument package. The more nearly horizontally isotropic the atmosphere, and the smaller the drift of the balloon, the larger the region over which the observation is representative. This paper focuses on the drift issue by presenting, for the first time, a comprehensive global climatology of radiosonde balloon drift statistics.

[1]NOAA Air Resources Laboratory, Silver Spring, Maryland, USA.
[2]I.M. Systems Group, Rockville, Maryland, USA.
[3]NOAA Center for Satellite Applications and Research, Camp Springs, Maryland, USA.

Copyright 2011 by the American Geophysical Union.
0148-0227/11/2010JD014891

1.1. GRUAN Issues

[4] This analysis was motivated by questions of practical concern for the Global Climate Observing System (GCOS) Reference Upper Air Network (GRUAN). The GRUAN is meant to provide upper air measurements of GCOS "essential climate variables," in accordance with the GCOS climate monitoring principles [*Global Climate Observing System* (*GCOS*), 2003], with a full characterization of measurement uncertainty, to support reliable long-term climate monitoring, provide an anchor for calibrating more globally complete observations from satellites and other networks, and enable comprehensive climate process studies [*Seidel et al.*, 2009]. Specific issues for GRUAN include the following four problems.

1.1.1. Uncertainty Characterization Using Measurements From Collocated Instruments

[5] A key feature of GRUAN is redundant observations of atmospheric profiles using different, complementary, nominally collocated measurements, combined to fully characterize the overall measurement uncertainty [*Immler et al.*, 2010]. However, in practice there is some separation between instruments, and it is important to ascertain how far apart measurement systems can be and yet be considered effectively to sample the same atmospheric column.

1.1.2. Enhanced Observations via Distributed Sites

[6] To achieve redundancy of measurements, several GRUAN station proposals call for amalgamating two or three existing "nearby" sites, with complementary atmospheric profiling systems, to form a single GRUAN site. However, such a distributed station is only of value to GRUAN if the

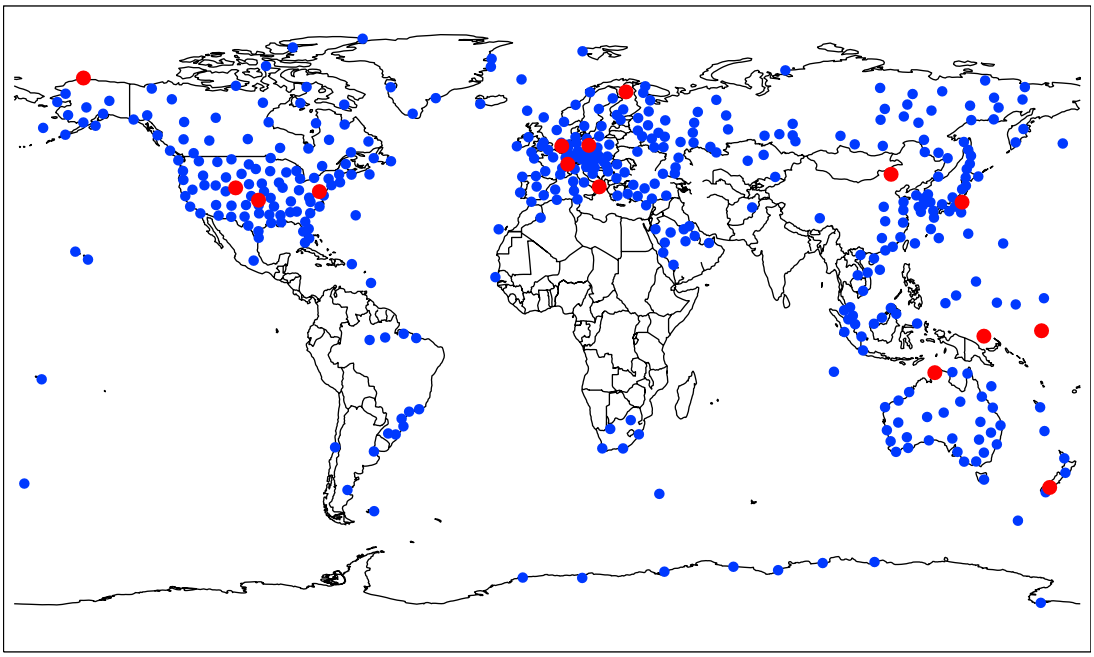

Figure 1. Global map of radiosonde stations used in this analysis, including GCOS Reference Upper Air Network sites (red).

additional uncertainty introduced by spatial separation does not cause the overall uncertainty to exceed specifications. The practical question is, "How far apart can subsites be and still be considered a single GRUAN site?"; and the answer may vary regionally, seasonally, vertically, by atmospheric parameter, and by instrument uncertainty.

1.1.3. Anchoring Satellite Data

[7] The long-term continuity and validation of satellite-derived atmospheric profile data products depend on ground-based measurements. With complete uncertainty characterization, GRUAN data can anchor globally complete satellite data, but only to the extent that both are representative of the same column of air. *Sofieva et al.* [2008] and *Pougatchev et al.* [2009] examined aspects of this problem, using more-frequent-than-usual radiosonde data from Sodankylä, Finland, and Lindenberg, Germany, respectively, to characterize the spatial structure function of atmospheric temperature (and humidity in the latter study). *Tobin et al.* [2006] and *Sun et al.* [2010] compared radiosonde data from the global network with satellite temperature, humidity and (in the latter case) refractivity profile observations and noted the importance of collocation criteria. *Sun et al.* [2010] quantified the increase in RMS differences with increasing spatial and temporal mismatches, taking into account both radiosonde drift and satellite displacements. However, none of these studies provide comprehensive analysis of radiosonde drifts for use in planning or evaluating protocols for using radiosonde data to anchor satellite observations.

1.1.4. Retrieval of Radiosonde Equipment

[8] Because of the need for high-quality temperature and humidity data from the surface through the lower stratosphere, GRUAN soundings are to be made with the best available, reference-quality instruments. To maximize the return on investment in these instruments, their retrieval and rehabilitation after flights is a priority. To plan the retrieval program, one must know how far and in what direction a reference radiosonde is likely to drift before falling back to ground.

1.2. Previous Studies

[9] This study addresses all of the four issues above by developing a comprehensive global climatology of balloon drift, which, to our knowledge, has not been developed before. However, *Houchi et al.* [2010] present a gross climatology of radiosonde drift distances, based on 1 year of high-vertical-resolution data from a limited set of stations in North America and the Northern Hemisphere Tropics, as part of a broader study of wind and wind shear. They present mean and median drift distance as a function of height for four climate zones. Median drift distances increase from the surface to 35 km, are lowest in the Tropics and highest in the Midlatitudes and Subtropics, and are less than 10 (35, 65) km below altitudes of 5 (10, 20) km [*Houchi et al.*, 2010, Figure 6].

[10] The lack of interest in drift statistics is probably because balloon drift is not of great concern in most radiosonde data applications, such as: assimilation of the observations into numerical weather prediction models with coarse horizontal resolution compared with the drift distance [*MacPherson*, 1995]; compilation of climate statistics for comparison with models or detection of trends [*McGrath et al.*, 2006]; and comparison of radiosonde and satellite-derived atmospheric profiles when the latter have large "footprints" [*Reale et al.*, 2008]. But to meet the GRUAN goal of providing climate reference observations of atmospheric profiles, balloon drift must be quantified.

[11] While we focus here on balloon drift, there is also a temporal aspect of some of the issues outlined above. Radiosondes take 1 to 2 h to reach their final heights, but

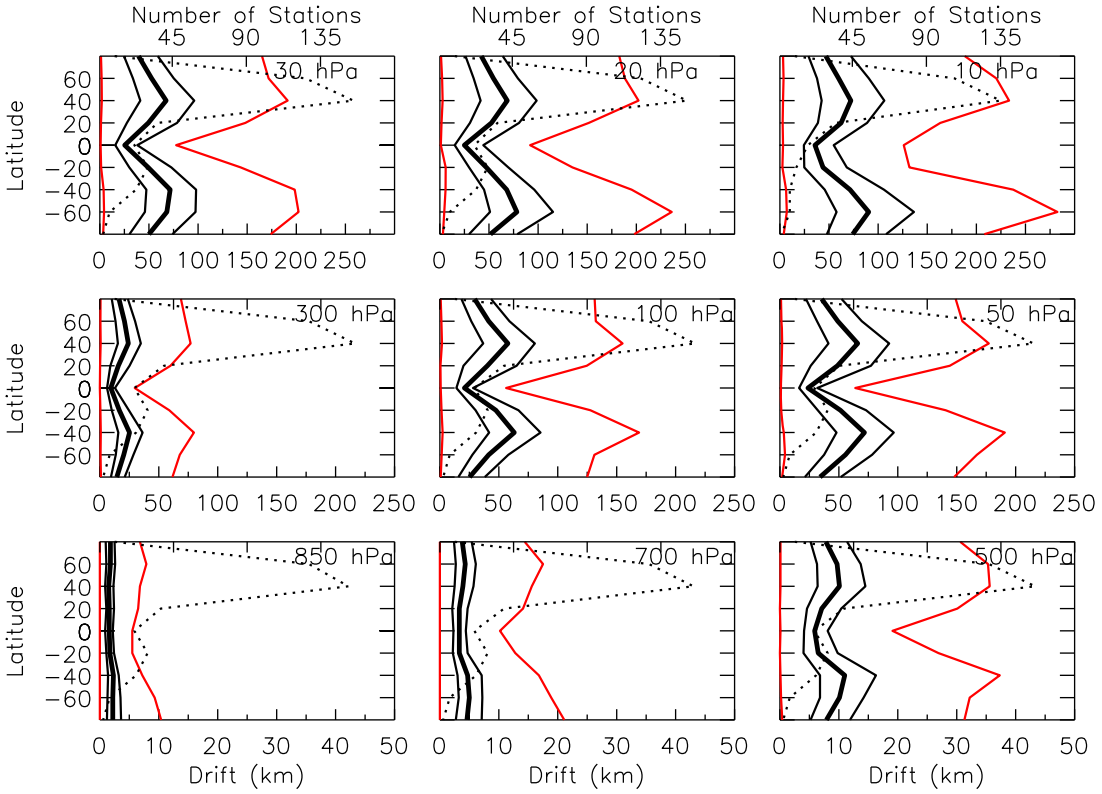

Figure 2. Zonal average values of minimum and maximum (red lines), and 25th, 50th, and 75th percentile (black lines) balloon drift distances for nine different pressure levels. Note the different horizontal scales used in each row. The number of stations contributing to the 20 degree latitude zonal average is shown by dotted black lines.

elapsed time depends on balloon ascent rate, which is often assumed to be constant but which may vary according to balloon type and inflation conditions (which can be controlled) and atmospheric vertical motion (which varies from sounding to sounding).

[12] Section 2 describes the data and methods used for the climatology. Section 3 presents global climatological balloon drift statistics, as a function of latitude, altitude, and season, and section 4 presents local results for each of the initial GRUAN stations. Section 5 provides basic results on balloon ascent time, to complement the drift distance climatology. Section 6 summarizes our main findings. Additional results, including an interactive software system, DriftPlotter, that allows users to select and view specialized results, are available as auxiliary material.[1]

2. Data and Methods

[13] This study is based on balloon drift data calculated from radiosonde observations by NOAA's National Centers for Environmental Prediction/Environmental Modeling Center (as described at http://www.emc.ncep.noaa.gov/mmb/data_processing/prepbufr.doc/balloon_drift_for_TPB.htm, Dennis Keyser, personal communication, 2009). Drift information as a function of height is given as the latitude, longitude, and time coordinates of the balloon, based on the reported wind sounding. Using the latitude and longitude of the station, we compute vertical profiles of drift distance (km) and direction from the launch location.

[14] We employ data for the 2 year period from July 2007 through June 2009 from 419 stations shown in Figure 1, which depicts the well-known Northern Hemisphere bias of the global radiosonde network. Stations were selected if at least 70% of the expected number of soundings were available in the NOAA Products Validation System [*Pettey et al.*, 2009], which includes archived radiosonde, satellite, and other vertical profile data. This analysis is based on a total of 552,962 radiosoundings, or an average of 1320 soundings per station.

[15] For each station, season (DJF, MAM, JJA, SON), and mandatory data reporting level (1000, 925, 850, 700, 500, 400, 300, 250, 200, 150, 100, 70, 50, 30, 20, and 10 hPa), we rank-order the computed balloon drift distances. These are used to create histograms of the probability distribution function of drift for the GRUAN candidate sites (Figure 1). For all stations, minimum, maximum, and 25th, 50th, and 75th percentile values of drift distance are determined from the ranked data. The same statistics are computed for full-year data, and for the final balloon height.

[16] For global and regional climatological analyses, the station statistics are displayed on contour maps. In addition, because they show much more variation in latitude than

[1] Auxiliary materials are available in the HTML: doi:10.1029/2010JD014891.

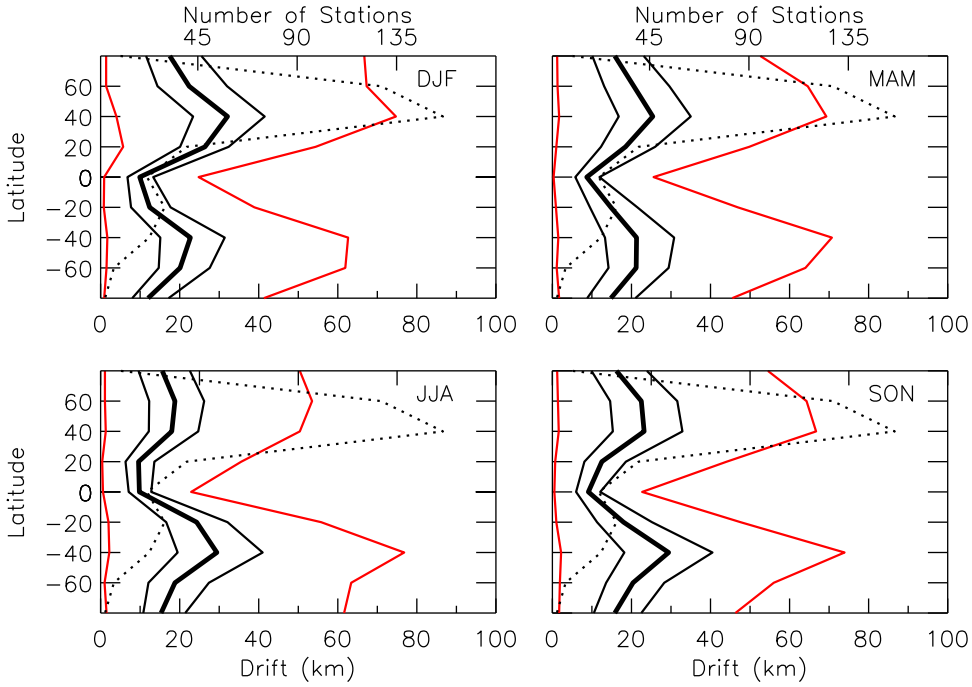

Figure 3. Zonal average values of minimum and maximum (red lines), and 25th, 50th, and 75th percentile (black lines) balloon drift distances at 300 hPa for each of the four seasons. The number of stations contributing to the 20 degree latitude zonal average is shown by dotted black lines. DJF, December–February; MAM, March–May; JJA, June–August; SON, September–November.

longitude, we have averaged them over 20 degree latitude bands to summarize the results in section 3.

3. Global Climatology of Balloon Drift Statistics

3.1. Height and Latitude Variations

[17] Figure 2 shows climatological, zonal mean balloon drift statistics for nine representative pressure levels (850, 700, 500, 300, 100, 50, 30, 20 and 10 hPa), based on all the soundings for the 2 year period analyzed. In addition to balloon drift distances, each panel in Figure 2 also shows the total number of stations in each 20 degree latitude band, ranging from fewer than 10 in the Southern Hemisphere polar zone to more than 200 in the Northern Hemisphere temperate zone.

[18] Each panel in Figure 2 shows the zonal average values (averaging over all stations in the zone) of the minimum and maximum, and 25th, 50th, and 75th percentile values of balloon drift distance. In the lower troposphere up to 500 hPa (Figure 2, bottom), balloon drift is always less than 40 km, with balloons drifting that far only in zones of the midlatitude storm tracks and only by 500 hPa. Median (50th percentile) values (thick black lines in Figure 2) are approximately 2 km at 850 hPa, 5 km at 700 hPa, and 6–11 km at 500 hPa, with interquartile ranges of about 2, 3, and 6 km, respectively.

[19] As the sondes ascend, the drift increases. In the upper troposphere (300 hPa), median values are about 15 km in the tropics and 25 km in midlatitudes, and in the lower stratosphere (50 hPa) they are 2 to 3 times greater. The latitudinal structure, with maxima in median drift distance (and larger ranges of drift distance) in the midlatitude zones of both hemispheres and a minimum (with smaller range) near the equator, reflects well-known zonal wind speed climatology [e.g., *Peixoto and Oort*, 1992, chapter 7]. The similarity of the drift distance values at the stratospheric 30, 20, and 10 hPa levels is due in part to the vertical shear in wind direction between levels, causing some balloons to drift back toward their launch locations. Note, however, that not all soundings achieve these low-pressure levels, so that the statistics at different levels are not derived from identical sets of soundings.

3.2. Seasonal Variations

[20] The results shown in Figure 2 were based on data for the full 2 year period. Figures 3 and 4 reveal seasonal variations in the drift distance statistics. Figure 3 shows zonal average drift distance statistics for 300 hPa for each of the four seasons. The global maps in Figure 4 show median values of the final drift distance (at sounding termination) for each season, to give a sense of the strongly zonal character of these results. (Comparable seasonal results for other pressure levels are presented in the accompanying auxiliary material.)

[21] The most striking features shown in Figures 3 and 4 are (1) the larger drift distances in midlatitudes in winter than in summer, with intermediate values in spring and fall and (2) the larger distances in Southern Hemisphere than in the Northern Hemisphere (also seen in Figure 2). The former feature is an expected result of well-known seasonal variations in prevailing (particularly jet stream) wind speeds. The latter may be due to the poorer sampling of

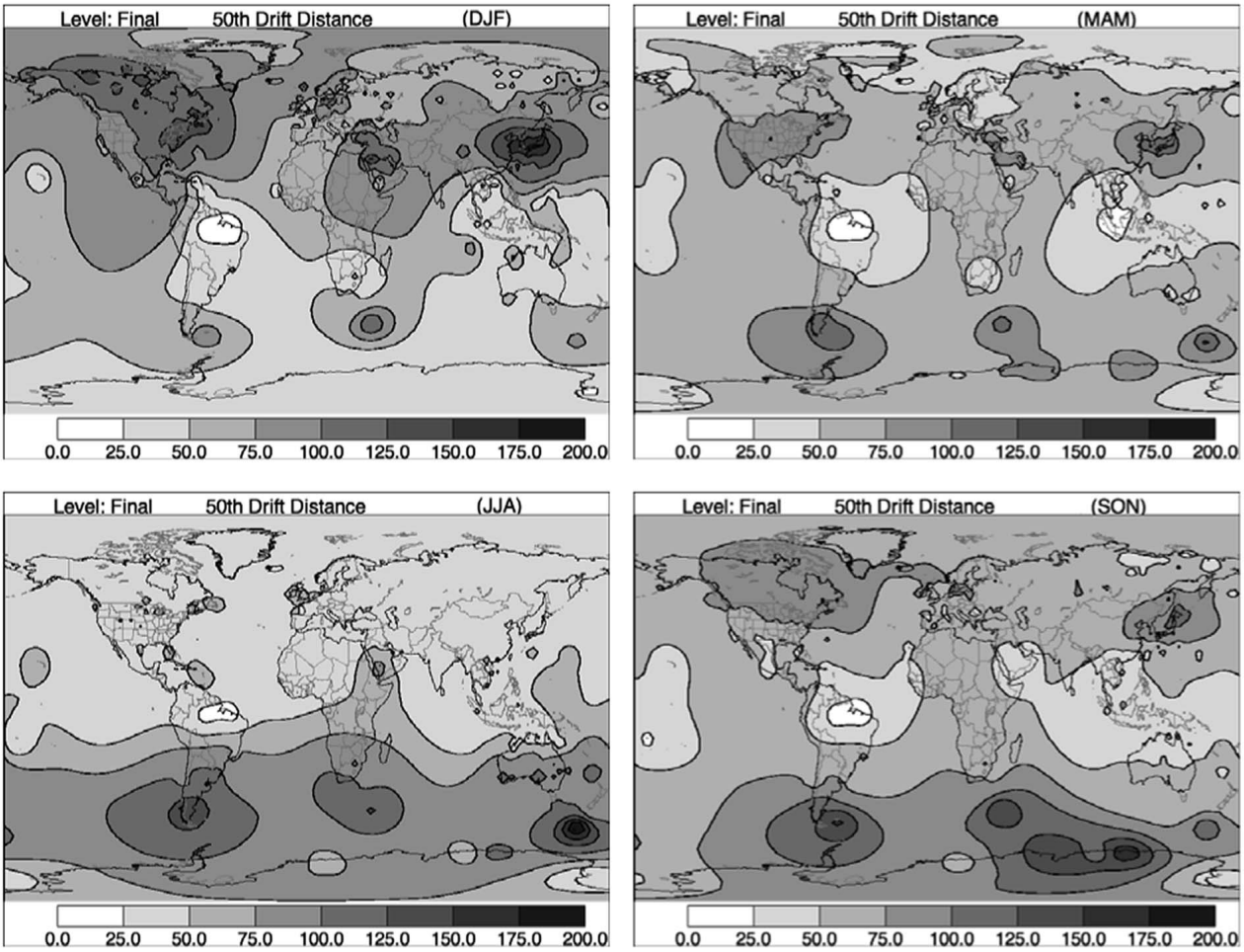

Figure 4. Global contour maps of median values of final balloon drift distance (kilometers) for each season. Contours are based on data from radiosonde stations shown in Figure 1; note the sparse sampling in the Southern Hemisphere.

Table 1. Stations Participating in the Global Climate Observing System (GCOS) Reference Upper Air Network (GRUAN) and, Where Appropriate, Nearby Associated Operational Radiosonde Stations and Partnering Stations and Approximate Separation Distance

GRUAN Station	Latitude	Longitude	Elevation (m)	Associated Operational Station	Separation (km)
Barrow, AK, USA	71.32°	−156.61°	8		
Beltsville, MD, USA	39.05°	−76.88°	53	Sterling, VA	50
Boulder, CO, USA[a]	39.95°	−105.20°	1743	Denver, CO	50
Cabauw, Netherlands	51.97°	4.92°	1	De Bilt	20
Darwin, Australia	−12.43°	130.89°	30		
Lamont, OK, USA	36.60°	−97.49°	320		
Lauder, New Zealand	−45.05°	169.68°	370	Invercargill	180
Lindenberg, Germany	52.21°	14.12°	98		
Manus, Papua New Guinea	−2.06°	147.42°	6		
Nauru, Nauru	−0.52°	166.92°	7		
Payerne, Switzerland	46.81°	6.95°	491		
Potenza, Italy	40.60°	15.72°	720	Brindisi	160
Sodankylä, Finland	67.37°	26.63°	179		
Tateno, Japan	36.06°	140.13°	31		
Xilin Hot, China	43.95°	116.12°	1013		

[a]The proposed GRUAN site at Boulder includes three subsites in Boulder within 11 km of each other and about 30–45 km from the Denver, CO, operational radiosonde station.

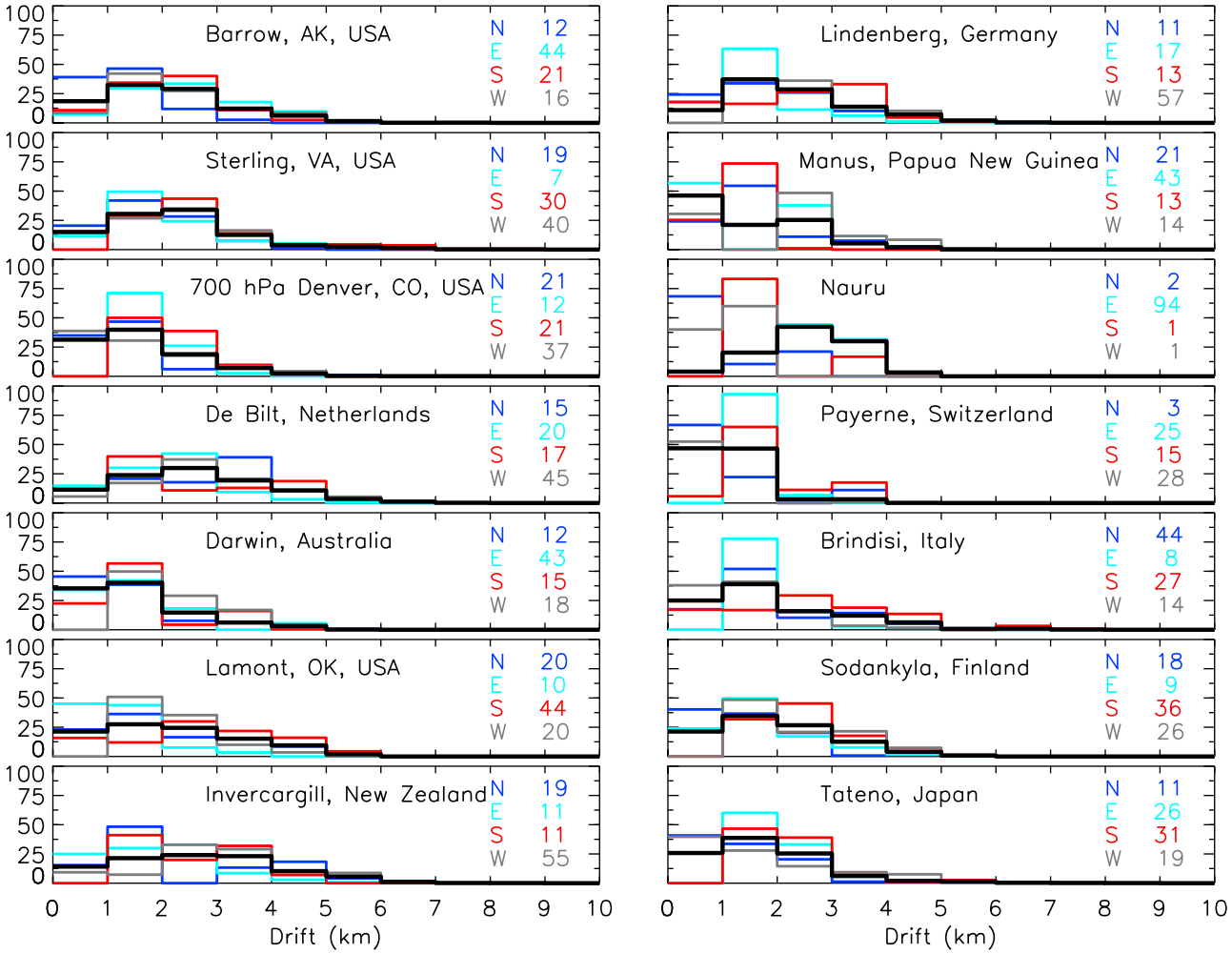

Figure 5. Histograms of the frequency of balloon drift distances (kilometers) at 850 hPa for 14 radiosonde stations, each collocated with or near a GRUAN site. Results based on all data are shown in black. Results segregated by wind direction are shown in colors. Color key indicates the percentage of winds from each of four directions (e.g., W indicates winds from within 45 degrees of west, or 225 to 315 degrees). Percentages do not always total 100 because cases of calm wind are not included in the direction-differentiated results.

the Southern Hemisphere (Figure 1), which also explains the irregular patterns of drift distance (Figure 4), and/or its greater fractional area covered by ocean, leading to higher wind speeds.

4. Balloon Drift Statistics for GRUAN Sites

[22] The results shown in section 3 gave typical balloon drift distances and their variability with height, season, and latitude. This section gives station-specific results meant to be directly applicable to decision-making for the GRUAN, as discussed in section 1. Table 1 gives the locations of operating or planned GRUAN sites and the location of the nearby operational radiosonde sites if a GRUAN site is not also an operational station.

[23] Figure 5 presents histograms of balloon drift distance for each operational station listed in Table 1, for 850 hPa (except for Denver, where we show 700 hPa results because of the high elevation of the station). We focus on 850 hPa to allow inferences to be made about the comparability of lower-tropospheric radiosonde data with measurements from ground-based remote-sensing profiling instruments (e.g., microwave radiometers) at the same site or nearby sites. Figure 6 shows comparable results for 50 hPa, to provide guidance to comparisons of radiosonde and, e.g., satellite data for the lower stratosphere. Results for other pressure levels are provided as auxiliary material, and some are discussed here.

[24] Almost all of the 850 hPa drift distances are ≤5 km, with modal values between 1 and 3 km at every station examined. At 500 hPa (not shown), drift distance rarely exceed 25 km, and modal values are between 5 and 15 km. These results show that balloon drifts within the troposphere are typically smaller than the substation separation distances (Table 1), so that balloons launched from one substation are very unlikely to sample the column directly over a part-

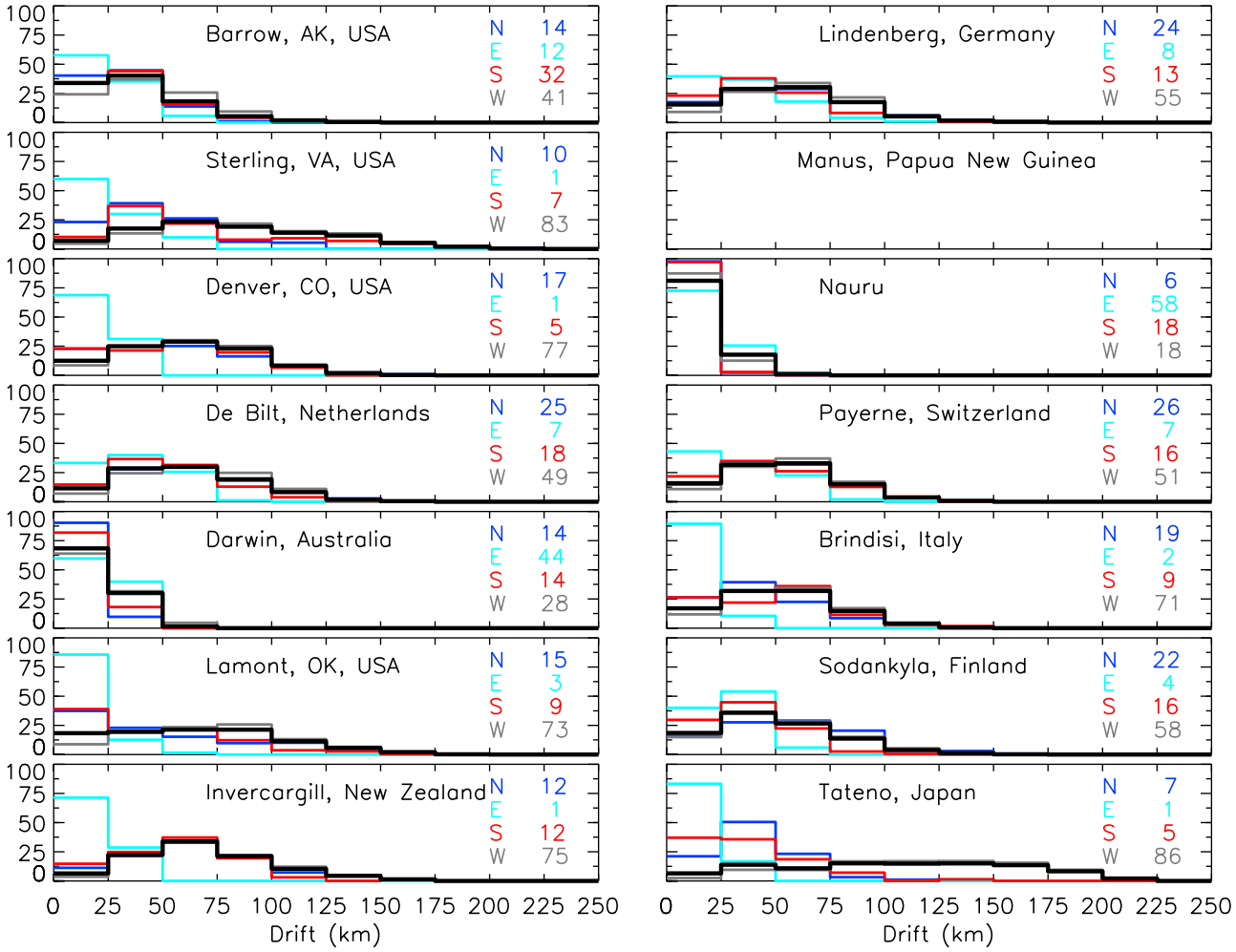

Figure 6. Same as Figure 5 but for 50 hPa. No results are shown for Manus, Papua New Guinea, due to limited sampling at 50 hPa at that station.

nering substation (even if they drifted in the direction of that substation). The interested reader is invited to examine animated maps of actual trajectories of radiosondes launched at or near GRUAN sites using the DriftPlotter software provided as auxiliary material.

[25] At 50 hPa (Figure 6), in the lower stratosphere, most drift distances are ≤125 km, with the exceptions of Tateno, Japan, and Sterling, Virginia, United States, where balloons have drifted as far as 200 km. The modal 50 hPa drift distances are typically between 25 and 75 km, although at the tropical stations (Nauru and Darwin, Australia) the balloons are rarely more than 25 km from the launch location.

[26] There is some dependence of drift distance on wind direction, because of the dependence of wind speed on direction in many locations. Figures 5 and 6 present histograms of drift distance for each of the four cardinal wind directions (±45°), excluding calm wind cases (speed < 1 knot = 1.85 km/h). Wind directions were computed from balloon location information at each level and therefore represent integration over the vertical column from the surface to the level in question. For example, at 850 hPa (Figure 5), southerly winds tend to carry balloons further than easterly winds at several midlatitude Northern Hemisphere stations, including Lamont, Oklahoma, United States (near the Southern Great Plains GRUAN site); Brindisi, Italy (near the Potenza GRUAN site); Denver, Colorado, United States (near the Boulder GRUAN site); Tateno, Japan; and Lindenberg, Germany (the GRUAN Lead Center).

5. Balloon Ascent Time

[27] As mentioned above, the spatial drift is one aspect of radiosoundings that is relevant to the problems outlined in section 1. Elapsed sounding time can also be a consideration for characterizing measurement uncertainty, anchoring satellite observations, and retrieving sounding equipment. Studies comparing satellite and radiosonde observations (and requiring radiosonde space and time coordinates for matching collocated observations) frequently estimate elapsed time using an assumed rate of balloon ascent.

[28] To assess the validity of this assumption, Table 2 provides global statistics of observed and estimated (using constant 5 and 6 m/s rise rates) elapsed sounding time for 9 standard pressure levels. Typical observed times for balloons to reach 850 hPa is <0.08 h (with a range of 0.06 to

Table 2. Average Statistics of Elapsed Time of Radiosonde Balloon Ascent From Launch to Selected Pressure Levels, Based on 552,962 Soundings Used in This Study, and Estimated Elapsed Time Assuming 5 and 6 m/s Balloon Rise Rates and U.S. Standard Atmosphere Heights of Pressure Levels[a]

	Elapsed Time (hours)						
	Observed					Estimated	
Pressure (hPa)	Minimum	25th	50th	75th	Maximum	6 m/s	5 m/s
850	0.06	0.07	0.07	0.07	0.08	0.07	0.08
700	0.14	0.15	0.16	0.16	0.17	0.14	0.17
500	0.27	0.29	0.30	0.31	0.32	0.25	0.31
300	0.44	0.49	0.50	0.51	0.53	0.42	0.51
100	0.65	0.88	0.89	0.90	0.92	0.55	0.65
50	0.87	1.12	1.13	1.14	1.16	0.75	0.90
30	1.02	1.30	1.31	1.32	1.34	0.95	1.14
20	1.14	1.44	1.45	1.47	1.49	1.10	1.32
10	1.43	1.69	1.71	1.73	1.76	1.43	1.73

[a]Statistics comprise minimum, maximum, and 25th, 50th, and 75th percentile values.

0.08 h, or 3.6 to 4.8 min), which is consistent with the estimated time of 0.07–0.08 h. They ascend to the mid-troposphere (500 hPa) in 0.3 h (18 min), and at this level the estimated time based on 5 m/s rise is less than the minimum observed value of 0.27 h, but the estimate based on 6 m/s rise is more consistent with observations. In the upper troposphere and lower stratosphere (300–100 hPa), median observed times are 0.50–0.89 h, and constant-rise-rate estimates are within the observed range (maximum minus minimum) but up to 40% lower than the observed median. At higher stratospheric levels (50, 30, 20 and 10 hPa), median observed elapsed times exceed 1 h, and the ranges are approximately 20 min. At these highest levels, estimated values using 5 m/s rise are generally lower than minimum observed values, and although those based on 6 m/s are more realistic they too are lower than typical observed values. In summary, observed elapsed time have about a 20% spread around their median values. Assuming constant rise rate both neglects that observed variability and underestimates the observations at levels above 850 hPa.

6. Summary

[29] Radiosonde balloon drift distance and elapsed time climatologies have been developed from global data from 419 stations for the period July 2007 through June 2009. This paper presented a sampling of the statistical results; a more complete set of information is presented as auxiliary material.

[30] Typical values of drift distance are a few km in the lower troposphere, ~5 km in the midtroposphere, ~20 km in the upper troposphere, and ~50 km in the lower stratosphere, although there is considerable variability. Drift distances tend to: increase with height above the surface, be larger in midlatitudes than in the tropics, be larger in winter than in summer, and vary with wind direction.

[31] Estimates of elapsed time from balloon launch to various pressure levels, due to vertical balloon rise, have median values increasing from about 5 min at 850 hPa to about 1.7 h at 10 hPa, with ranges of about 20% of median values. Observed elapsed times exceed those estimated using assumed 5 or 6 m/s rise rates.

[32] **Acknowledgments.** We thank Daewon Byun and Tilden Meyers (NOAA Air Resources Laboratory), Peter Thorne (NOAA Cooperative Institute for Climate and Satellites), and three anonymous reviewers for useful reviews of this manuscript. Franz Immler (Deutscher Wetterdienst) provided helpful insight on applications of the results. The contents of this paper do not constitute a statement of policy, decision, or position on behalf of NOAA or the U.S. Government.

References

Global Climate Observing System (GCOS) (2003), The second report on the adequacy of the Global Observing Systems for Climate in support of the UNFCCC, *WMO Tech. Doc. 1143*, 85 pp., Geneva, Switzerland.

Houchi, K., A. Stoffelen, G. J. Marseille, and J. de Kloe (2010), Comparison of wind and wind-shear climatologies derived from high-resolution radiosondes and the ECMWF model, *J. Geophys. Res.*, *115*, D22123, doi:10.1029/2009JD013196.

Immler, F., J. Dykema, T. Gardiner, D. N. Whiteman, P. W. Thorne, and H. Vömel (2010), A guide for upper-air reference measurements, *Atmos. Meas. Tech. Discuss.*, *3*, 1807–1842, doi:10.5194/amtd-3-1807-2010.

MacPherson, B. (1995), Radiosonde balloon drift—Does it matter for data assimilation?, *Meteorol. Appl.*, *2*, 301–305, doi:10.1002/met.5060020402.

McGrath, R., T. Semmler, C. Sweeney, and S. Wang (2006), Impact of balloon drift errors in radiosonde data on climate statistics, *J. Clim.*, *19*, 3430–3442, doi:10.1175/JCLI3804.1.

Peixoto, J. P., and A. H. Oort (1992), *Physics of Climate*, 520 pp., Am. Inst. of Phys., College Park, Md.

Pettey, M., B. Sun, and T. Reale (2009), The NOAA PROducts (integrated) Validation System (NPROVS) and Environmental Data Graphical Evaluation (EDGE) Interface: Part-1: System, paper presented at 25th Conference on International Interactive Information and Processing Systems (IIPS) for Meteorology, Oceanography and Hydrology, Am. Meteorol. Soc., Phoenix, Ariz. (Available at http://ams.confex.com/ams/89annual/techprogram/paper_147823.htm)

Pougatchev, N., T. August, X. Calbet, T. Hultberg, O. Oduleye, P. Schlüssel, B. Stiller, K. S. Germain, and G. Bingham (2009), IASI temperature and water vapor retrievals–error assessment and validation, *Atmos. Chem. Phys. Discuss.*, *9*, 7971–7989, doi:10.5194/acpd-9-7971-2009.

Reale, A., F. Tilley, M. Ferguson, and A. Allegrino (2008), NOAA operational sounding products for ATOVS, *Int. J. Remote Sens.*, *29*(16), 4615–4651, doi:10.1080/01431160802020502.

Seidel, D. J., et al. (2009), Reference upper-air observations for climate: Rationale, progress, and plans, *Bull. Am. Meteorol. Soc.*, *90*, 361–369, doi:10.1175/2008BAMS2540.1.

Sofieva, V. F., F. Dalaudier, R. Kivi, and E. Kyrö (2008), On the variability of temperature profiles in the stratosphere: Implications for validation, *Geophys. Res. Lett.*, *35*, L23808, doi:10.1029/2008GL035539.

Sun, B., A. Reale, D. J. Seidel, and D. C. Hunt (2010), Comparing radiosonde and COSMIC atmospheric profile data to quantify differences among radiosonde types and the effects of imperfect collocation on comparison statistics, *J. Geophys. Res.*, *115*, D23104, doi:10.1029/2010JD014457.

Tobin, D. C., H. E. Revercomb, R. O. Knuteson, B. M. Lesht, L. L. Strow, S. E. Hannon, W. F. Feltz, L. A. Moy, E. J. Fetzer, and T. S. Cress (2006), Atmospheric radiation measurement site atmospheric state best estimates for Atmospheric Infrared Sounder temperature and water vapor validation, *J. Geophys. Res.*, *111*, D09S14, doi:10.1029/2005JD006103.

M. Pettey and B. Sun, I.M. Systems Group, 6309 Executive Blvd., Rockville, MD 20852, USA.

A. Reale, NOAA Center for Satellite Applications and Research, 5200 Auth Rd., Camp Springs, MD 20746, USA.

D. J. Seidel, NOAA Air Resources Laboratory, Silver Spring, MD 20910, USA. (dian.seidel@noaa.gov)